



Plasticity of single-grain icosahedral Al–Pd–Mn quasi-crystals deformed at room temperature

F. Momprou *, D. Caillard

CEMES-CNRS, 29, Rue Marvig, BP4347, F-31055 Toulouse Cedex, France

Received 10 December 2003; received in revised form 14 April 2004; accepted 15 April 2004

Available online 14 May 2004

Abstract

Transmission electron microscopy observations have been performed on icosahedral Al–Pd–Mn quasi-crystal samples deformed at 20 °C under a high confining pressure. They reveal a large density of wavy walls from which several climbing dislocations are emitted. Near-screw dislocations have been found at the wall terminations with a Burgers vector contained in the wall plane. Careful plane determinations and dislocation analyses are not consistent with a glide and cross-slip mechanism. The results can be better interpreted as a deformation by cracks in mode III followed by a re-healing process.

© 2004 Acta Materialia Inc. Published by Elsevier Ltd. All rights reserved.

1. Introduction

Since the demonstration has been done that dislocations are responsible for the plasticity of icosahedral quasi-crystals [1], many transmission electron microscopy (TEM) observations have been performed on Al–Pd–Mn single-grains after (post-mortem [2]), and during (in situ [3,4]) deformation. From these and further experiments, the idea had rapidly emerged that dislocations move essentially by glide, their motion being controlled by the crossing of clusters or the Peierls potential [5,6]. However, no clear experimental evidence of such a motion has been put forward as Burgers vectors and planes of motion could not be determined simultaneously. Climb was later on also considered but only as a restoration mode taking place at high temperature [7].

The idea that climb could be the dominant mode of motion came out recently from observations of the as-grown material [8–10], of deformed samples at 300 °C under a high confining pressure [11], and from in situ experiments [12]. In those experiments, planes of motion and Burgers vectors have been determined indepen-

dently, as a result only evidence of climb could be obtained. Under such conditions, the question has been raised whether glide is also possible, especially at very low temperature, where climb is a priori of disadvantage with respect to glide. In particular, Texier et al. [13] claim that plastic deformation of Al–Pd–Mn at room temperature under a high confining pressure generates pile-ups of dislocations moving by glide. To estimate the contribution of glide to low temperature plasticity, new experiments have been carried out in Al–Pd–Mn single-grains deformed at room temperature, under confining pressure. The experimental procedure is described first. Then, the results of TEM observations are analysed and discussed.

2. Experimental

A cylindrical sample of an Al_{70.1}Pd_{20.4}Mn_{9.5} single-grain (3 mm diameter, 3 mm height) has been deformed along the [0/1, 0/0, 1/0]¹ 5-fold direction in a multianvil apparatus at the “Laboratoire Magmas et Volcans” in Clermont–Ferrand. The specimen has been compressed at room temperature in a high pressure cell designed to generate high differential compressive stress, probably of

* Corresponding author. Tel.: +33-562-257-872; fax: +33-562-257-999.

E-mail address: momprou@cemes.fr (F. Momprou).

¹ In the notation of Cahn et al. [14].

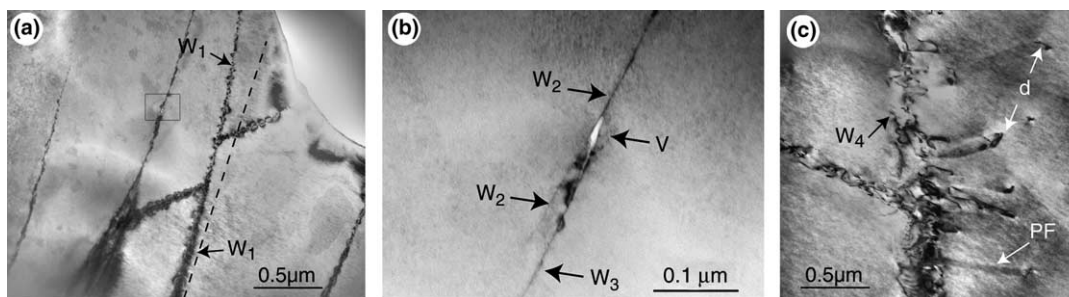


Fig. 1. General overview of samples deformed at 20 °C: (a) three-dimensional network of non-planar walls (W_1) concentrating a high density of defects. A void (V) at the intersection of two walls (W_2 , W_3) is enlarged in (b); (c) emission of dislocations (d) trailing phason faults (PF) by a wall (W_4).

the order of several 100 MPa. A pressure of 5 GPa is first raised and maintained during 2 h, before a slow decompression over 14 h. After a total deformation of a few percent, the specimen is still cylindrical. Slices have been cut 45° away from the (0/1, 0/0, 1/0) 5-fold plane perpendicular to the compression axis labelled C in the following. Samples were then thinned by conventional ion milling under cooling. They have been observed in a JEOL 2010 HC electron microscope operating at 200 kV, under two beam conditions, using the usual τ -related diffraction vectors $[20,32]$ and $[52,84]$ ² along 2-fold directions, noted $g_{2i(1)}$ and $g_{2i(2)}$, and the usual strong reflection $[18,29]$ along the 5-fold direction, noted g_{5i} . Large-angle convergent beam electron diffraction (LACBED) analyses have been carried out in a Phillips CM 30 operating at 300 kV in nanoprobe mode (for details see [10]).

3. Observations and interpretation

3.1. General observations

Fig. 1 shows the general features of samples deformed at 20 °C. Walls containing a high density of defects can be seen (Fig. 1(a)). They exhibit complex contrasts indicating that they contain high strain and stress concentrations. They are usually slightly non-planar, as indicated by their wavy traces at the surfaces, but close to 2-fold planes. For instance, the wall noted W_1 and seen edge-on in Fig. 1(a) deviates significantly from a 2-fold plane trace (dashed line). Misorientations across the walls are smaller than 1°. As shown in Fig. 1(a), walls are interconnected and form three-dimensional structures. Fig. 1(b) is an enlargement of the inset in Fig. 1(a) showing a void (V) at an intersection of two walls noted W_2 and W_3 . Fig. 1(c) shows a few dislocations, noted d , emitted from the wall noted W_4 , and

trailing the characteristic fringe pattern of phason faults (noted PF). These dislocations are not very frequently observed. They are described in the following section.

3.2. Dislocation emission

Several dislocations emitted by walls have been observed and analysed. Fig. 3 shows one of them trailing a phason fault under various contrast conditions in a sample sliced 45° away from the (0/1, 0/0, 1/0) 5-fold plane perpendicular to the compression axis. All the following notations refer to the stereographic projection of Fig. 2. Rules of contrast have been established for perfect dislocations by Wollgarten et al. [15] and specified for imperfect dislocations and phason faults by Momprou et al. [11]. In the latter case, the Burgers vector of the dislocation is completely defined by its Burgers vector in the physical space ($\mathbf{b}_{//}$), and the corresponding phason fault is defined by its displacement vector $\mathbf{r}_{//} = \mathbf{b}_{//}$, as a stacking fault in a crystal. Phason

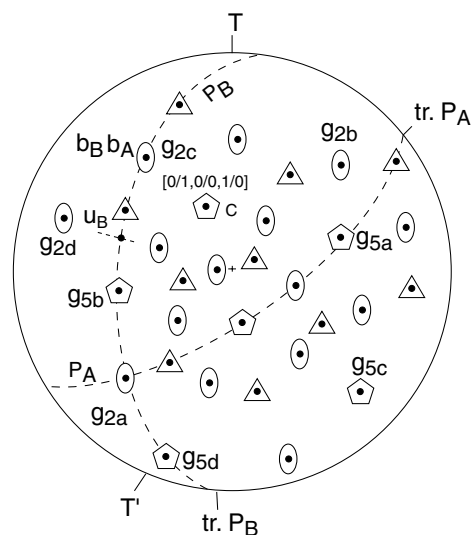


Fig. 2. Stereographic projection of the deformed sample. C refers to the compression axis; T and T' are the tilt axes used in TEM observations.

² $[N, M]$ is related to the modulus of the corresponding diffraction vector of the six-dimensional lattice, i.e., $G^2 = N + M\tau$ with τ the golden mean.

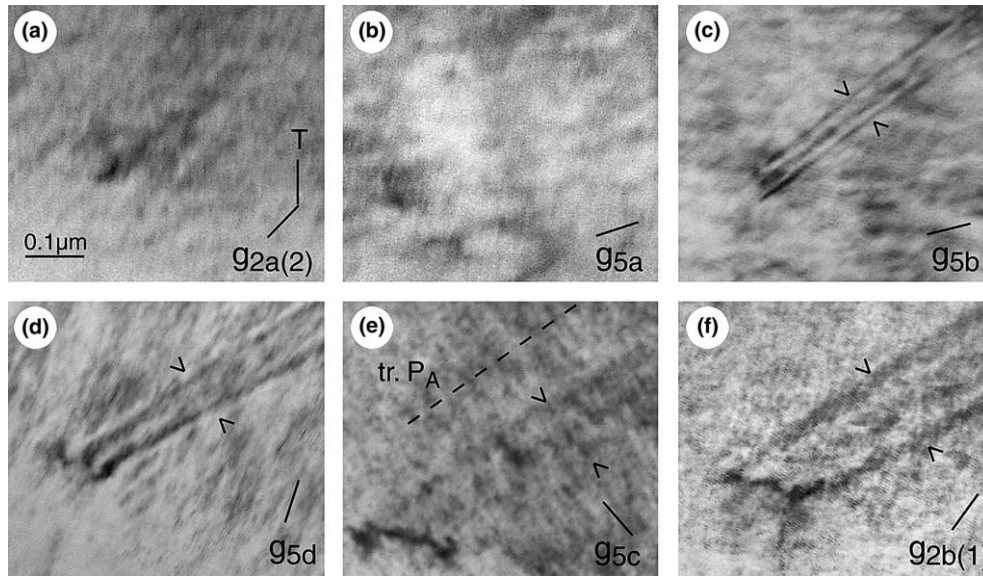


Fig. 3. Contrast analysis of an imperfect dislocation emitted by a wall. The dislocation and the fringes are out of contrast in (a) and (b). Only fringes are visible in (c) and (d). The outer fringes (dark or bright) are labelled by arrows.

faults exhibit a classical fringe pattern in inclined planes. Extinction conditions for the dislocation and the fault, which correspond to the condition $\mathbf{g}_{//} \cdot \mathbf{b}_{//} = 0$, have been obtained with \mathbf{g}_{2a} and \mathbf{g}_{5a} (Fig. 3(a) and (b)). The fringes of the fault are visible in all other situations. This unambiguously shows that $\mathbf{b}_{//}$ is parallel to the 2-fold direction perpendicular to \mathbf{g}_{2a} and \mathbf{g}_{5a} , noted \mathbf{b}_A in Fig. 2. Additional information can be obtained considering that the dislocation exhibits a single contrast in \mathbf{g}_{5c} and $\mathbf{g}_{2b(1)}$ (Fig. 3(e) and (f), respectively). As shown in Table 1, the Burgers vector is most probably $\mathbf{b}_{A//} = [\bar{1}/1, \bar{2}/1, \bar{3}/2]$, of length $b_{A//} = 0.183$ nm. The very faint dislocation contrast with \mathbf{g}_{5b} and \mathbf{g}_{5d} (Fig. 3(c) and (d)) corresponds to the “pseudo-weak” extinction described by Momprou et al. [11]. From its trace direction (tr. P_A) and the variation of its apparent width as a function of tilt angle, the phason fault plane P_A is found parallel to the $(1/1, 0/\bar{1}, 1/0)$ 2-fold plane perpendicular to the direction of the Burgers vector (Fig. 2). Thus, the dislocation has moved in this plane by pure climb.

3.3. Dislocations at wall terminations

When the walls are sufficiently close to the foil plane, dislocations are clearly seen at their terminations, and their contrast can be analysed. Farther, only broad contrasts and moiré-type contrasts can be seen which cannot be interpreted easily. Fig. 4 shows a complete analysis of the first 10 dislocations at a wall end. The dislocations are close to each other and no phason fault can be seen between them. All dislocations exhibit the same contrast and thus have the same Burgers vector. Extinction conditions have been obtained with \mathbf{g}_{2a} and \mathbf{g}_{5a} (Fig. 4(a) and (b), respectively). Single contrasts can be observed with \mathbf{g}_{5b} and \mathbf{g}_{5c} (Fig. 4(c) and (d)) and double contrasts (arrowheads) can be observed with, $\mathbf{g}_{2c(2)}$ and $\mathbf{g}_{2d(2)}$ (Fig. 4(e) and (f)). This leads to a 2-fold Burgers vector $\mathbf{b}_{B//} = [1/0, 1/\bar{1}, 2/\bar{1}]$ of length $b_{B//} = 0.296$ nm (Table 2). The wall plane seems to be slightly wavy because its apparent width is not constant and because it does not end at the foil surface along

Table 1

Contrast conditions for dislocations with a Burgers vector $\mathbf{b}_{A//} = [\bar{1}/1, \bar{2}/1, \bar{3}/2]$

\mathbf{g}	$\mathbf{g}_{//}$	$\mathbf{g}_{//} \cdot \mathbf{b}_{A//}$	$\mathbf{G} \cdot \mathbf{B}_A$	Fig. 3	Contrast
$\mathbf{g}_{2a(1)}$	$1/2, 1/1, \bar{2}/\bar{3}$	0	0		E
$\mathbf{g}_{2a(2)}$	$2/3, 1/2, \bar{3}/\bar{5}$	0	0	(a)	E
\mathbf{g}_{5a}	$0/0, 1/2, 2/3$	0	0	(b)	E
\mathbf{g}_{5b}	$2/3, 0/0, \bar{1}/\bar{2}$	0.44	0	(c)	PWE
\mathbf{g}_{5d}	$0/0, 1/2, 2/3$	-0.44	0	(d)	PWE
\mathbf{g}_{5c}	$\bar{1}/\bar{2}, 2/3, 0/0$	-0.72	-1	(e)	S
$\mathbf{g}_{2b(1)}$	$0/0, 0/0, 2/4$	0.26	1	(f)	S

S – single contrast, E – extinction, PWE – pseudo weak extinction.

$\mathbf{G} \cdot \mathbf{B}_A$ would be the phase shift if retiling was possible.

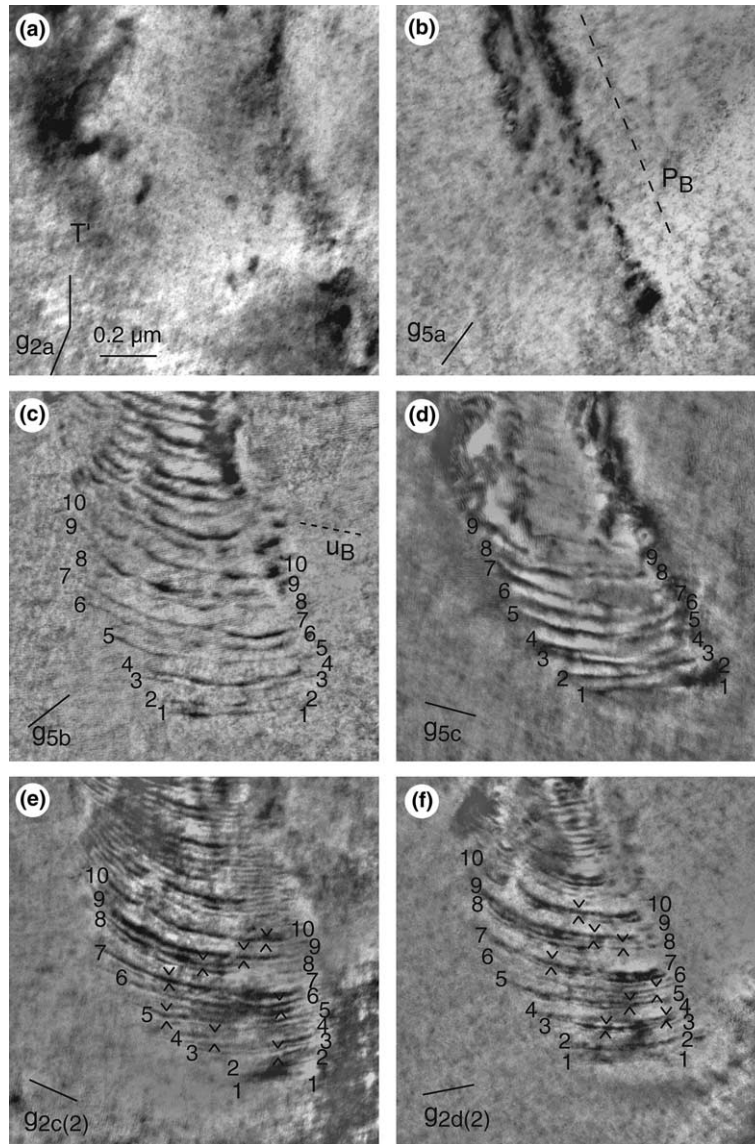


Fig. 4. Contrast analysis of the first ten dislocations at a wall termination. Double contrast conditions are observed in (e) and (f) (arrowheads).

Table 2

Contrast condition for dislocation with a Burgers vector $\mathbf{b}_{B//} = [1/0, 1/\bar{1}, 2/\bar{1}]$

\mathbf{g}	$\mathbf{g}_{//}$	$\mathbf{g}_{//} \cdot \mathbf{b}_{B//}$	$\mathbf{G} \cdot \mathbf{B}_B$	Fig. 4	Contrast
$\mathbf{g}_{2a(1)}$	$1/2, 1/1, \bar{2}/\bar{3}$	0	0	(a)	E
$\mathbf{g}_{2a(2)}$	$2/3, 1/2, \bar{3}/\bar{5}$	0	0		E
\mathbf{g}_{5a}	$0/0, 1/2, 2/3$	0	0	(b)	E
\mathbf{g}_{5b}	$2/3, 0/0, \bar{1}/\bar{2}$	0.72	1	(c)	S
\mathbf{g}_{5c}	$\bar{1}/\bar{2}, 2/3, 0/0$	-1.17	-1	(d)	S
$\mathbf{g}_{2c(2)}$	$3/5, 2/3, 1/2$	2.34	2	(e)	D
$\mathbf{g}_{2d(2)}$	$3/5, 2/3, \bar{1}/\bar{2}$	1.89	2	(f)	D

S – single contrast, E – extinction, D – double contrast.

rectilinear directions. However, average trace directions and apparent widths as a function of the tilt angle correspond to the $(1/0, 1/1, 0/1)$ 2-fold plane which contains the Burgers vector (see Fig. 2). Since the dislocations are in average parallel to the dense pseudo 2-fold direction \mathbf{u}_B (Fig. 2), they have near-screw character.

3.4. LACBED analysis

Far away from the head, the contrast of the walls cannot be interpreted easily. However, the LACBED technique provides additional information. In Fig. 5(a), a wall (W) is seen edge-on along the direction marked by

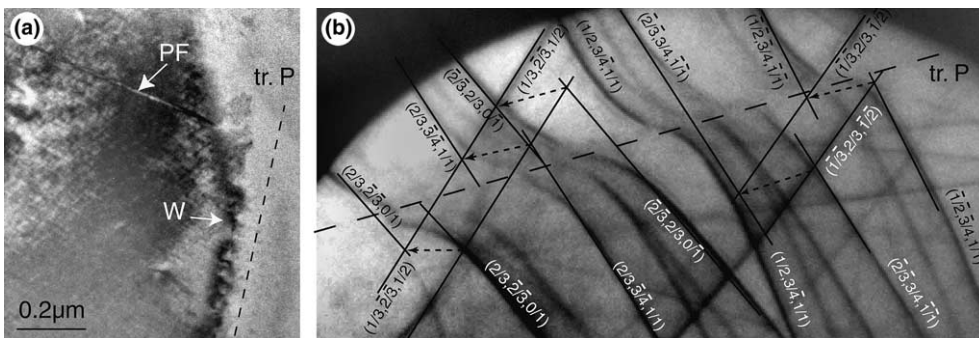


Fig. 5. Results of LACBED experiments: (a) edge-on wall, W; (b) corresponding shift of the Bragg's lines in a direction parallel to the wall plane.

a dashed line. A phason fault (PF) emerges from it as a result of the emission of a dislocation. Fig. 5(b) shows that the Bragg lines are shifted when they cross the wall and that the shift between corresponding intersecting points of Bragg lines (dashed arrows) is constant. This shift is directly related to the rotation across the two half parts of the wall. Since it is parallel to the trace of the wall, the rotation has taken place in the wall plane, namely around a direction perpendicular to the wall. In other words, the wall is like a twist boundary.

3.5. Evaluation of possible cross-slip activity

This section is based on the description of a long wall almost contained in the foil plane, shown in Fig. 6. It contains a high density of dislocations and exhibits a variable apparent width corresponding to a variable foil thickness. It is non-planar and can be considered as

made of three distinct planes noted P_1 , P_2 and P_3 , with respective traces tr. P_1 , tr. P_2 and tr. P_3 . The apparent widths of P_1 , P_2 and P_3 have been measured as a function of tilt angle in four different imaging conditions (Fig. 6(a)–(d)). The widths are plotted in Fig. 7(a) as a function of the tilt angle and fitted with the curves corresponding to the planes shown in Fig. 7(b) and going through tr. P_1 , tr. P_2 and tr. P_3 . The error bars on the directions of the three plane normals (\mathbf{n}_1 , \mathbf{n}_2 , \mathbf{n}_3) correspond

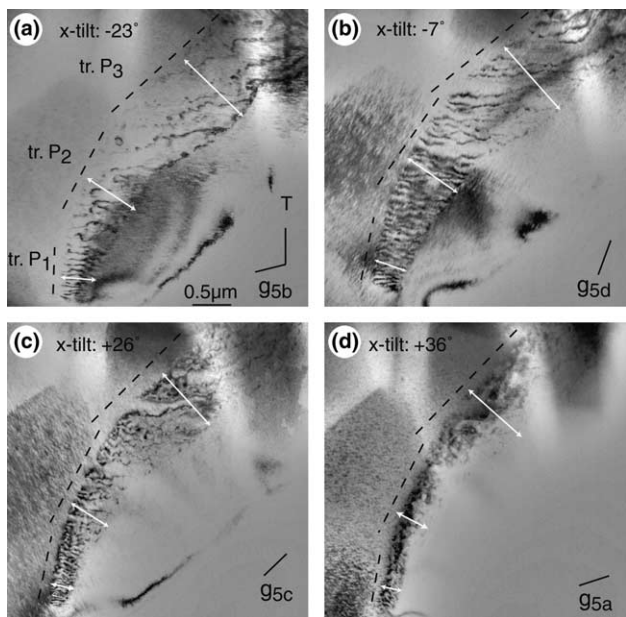


Fig. 6. Analysis of a wavy wall containing a large dislocation density. Dashed lines indicate the traces of its three different habit planes (P_1 , P_2 and P_3). White arrows indicate the apparent widths of P_1 , P_2 and P_3 under different tilt angles.

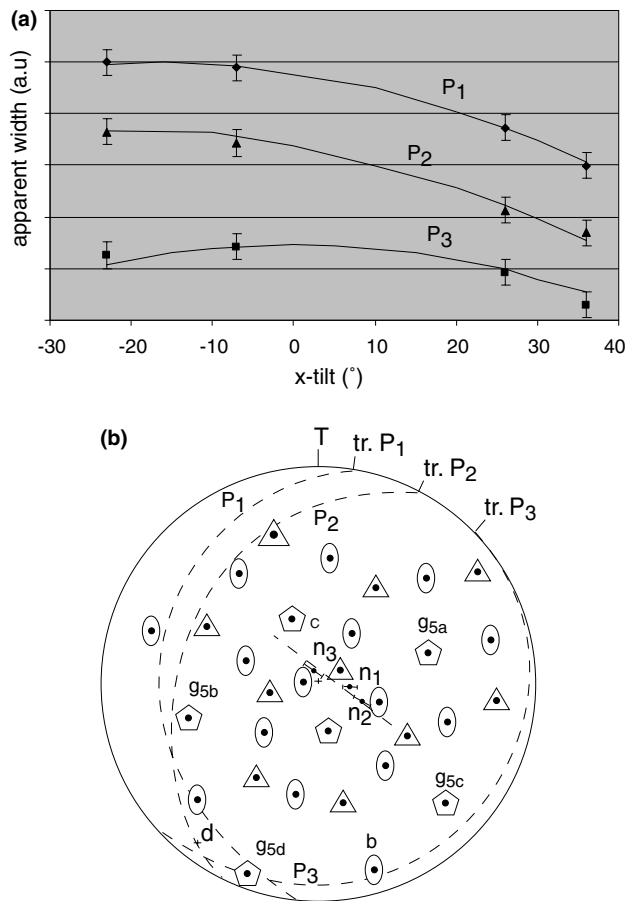


Fig. 7. (a) Variation of the apparent width of planes P_1 , P_2 and P_3 as a function of x -tilt angle around the tilt direction T . Curves going through experimental points correspond to the planes shown in (b).

to the uncertainty of the width measurements. P_1 is almost parallel to the (1/0, 1/1, 0/1) 2-fold plane, P_3 to the (1/1, 0/1, 1/0) 2-fold one and P_2 has an intermediate position. The three planes intersect approximately along a direction noted d which is not a dense direction. The dislocations have been tentatively studied by contrast analysis. Although a clear Burgers vector determination was not possible, it appears that several different Burgers vectors are present in the three planes. Indeed, the number and the aspect of visible dislocations are clearly different from one imaging condition to another one. Comparing the density of visible dislocations in the planes P_1 , P_2 and under the four imaging conditions (Fig. 6(a)–(d)) shows that the dislocations have at least two different Burgers vectors. For instance, a lower density of dislocations is observed with g_{5b} , compared to g_{5c} (Fig. 6(a) and (c), respectively) while all the dislocations are out of contrast in g_{5a} (Fig. 6(d)). This suggests that at least one Burgers vector is along the direction perpendicular to g_{5b} and g_{5a} , noted b , different from d (see Fig. 7(b)). Then, even if each part of the wall could be formed by a glide process, the wavy aspect of the whole structure cannot be explained by glide and cross-slip because cross-slip would require that all Burgers vectors are contained in all planes of motion.

4. Discussion

The observation of dislocation motion by climb at room temperature is surprising considering that the corresponding diffusion rate must be extremely small. However, mechanical tests revealed that the activation energy decreases substantially with increasing stresses [16]. At low temperature, but under the huge stresses due to strain incompatibilities under high confining pressure, the activation energy may thus be significantly lower than at high temperature, and still allows for some climb motion. The possible origin of the decrease in activation energy with increasing stress will be discussed in another article.

Samples deformed at 300 °C exhibit the same common features, i.e., the presence of deformation walls from which individual dislocations have been emitted by climb, although a larger density of climbing dislocations has been observed [11].

Observations of dislocations at wall terminations, with Burgers vectors parallel to the wall planes, confirm the previous investigation of Texier et al. [13]. However, contrary to those authors, we do not conclude that they result from a glide mechanism, because the inspection of wavy walls has shown that they cannot be formed by a glide plus cross-slip mechanism. Wall formation can be interpreted in a more coherent way by a crack and healing mechanism. Deformation occurs first by non-planar cracking followed by a re-healing assisted by the

hydrostatic pressure. In the situation described here, cracks are produced principally in mode III, i.e., by a rotation around a direction located at the crack tip and perpendicular to the crack plane. This conclusion is consistent with: (i) the results of LACBED experiments, and (ii) an accommodation by screw dislocations at the crack head (note that a second family of screw dislocations would be necessary to form a twist boundary with no long-range stress).

Similar observations have been made in silicon wafers bonded after a relative rotation perpendicular to the interface plane [17]. Cracking and re-healing has also been observed in indented silicon [18,19] and in sapphire where dislocation networks and moiré contrasts have been found near arrested crack tips [20]. Dislocation networks have also been observed in scratched sapphire submitted to impulse loading by Wiederhorn et al. [21] and interpreted as the result of spontaneous crack healing. In the present observations, voids at the junctions between two walls support the idea of a crack process with imperfect re-healing where high strain incompatibilities occur. The fact that the microstructure far from the crack tip is more and more complex can be interpreted by considering that crack surfaces are not planar. Then, after rotation, the two surfaces of the cracks do not match perfectly, especially away from the crack head, which induces strong local strains and associated stresses. Too high stresses can however relax by emission of climbing dislocations trailing phason faults. Close to the crack head, on the contrary, the two surfaces can be more perfectly sealed and rotation can be accommodated by screw dislocations. A single-grain of Al–Pd–Mn quasi-crystal indented at low temperature by Wollgarten et al. [22] shows a poly grained microstructure which exhibits similar features: bending contours and dislocations originating from numerous cracks. The authors interpreted their results as grain boundary sliding, but indicated that cold welding may participate to connect cracks. Cross-sectional observations of diamond scratches in icosahedral Al–Pd–Mn also showed the presence of partially connected cracks beneath the scratch [23].

Another point that must be discussed is the absence of phason faults in the wake of dislocations at the head of the crack. This feature is not easily observed in our experiments, but it appears clearly in those of Texier et al. [13]. As a fringe contrast should be observed in case of a glide (or climb) mechanism, its absence confirms that the walls originate from another process. This can be explained assuming that only a part of the relative rotation between the two lips is accommodated by dislocations. Then, in contrast to what occurs in case of a glide or climb mechanism, the displacement vector across the plane of the cut would not be uniform between adjacent dislocations. This would result in a complex variation of the phase shift which could not yield the usual fringe contrast.

5. Conclusions

TEM observations of samples deformed at room temperature have yielded the following results:

- The deformation results from the formation of a network of non-planar walls. Walls exhibit a complex contrast in general and a dislocation-like contrast at their terminations. They emit climbing dislocations.
- The observation of climb at such a low temperature shows that the corresponding activation energy must decrease substantially with increasing stress.
- The geometry of walls and the nature of dislocations at their terminations are inconsistent with a formation by a glide and cross-slip mechanism.
- Walls are proposed to be the result of a deformation by crack and subsequent re-healing assisted by the hydrostatic pressure. Re-healing results in the formation of the observed dislocations.

Acknowledgements

We greatly acknowledge Y. Calvayrac for the difficult growth of Al–Pd–Mn samples, and P. Cordier and L. Bresson for the sample deformation at Laboratoire Magmas et Volcans in Clermont–Ferrand.

References

- [1] Wollgarten M, Beyss M, Urban K, Liebertz H, Kocster U. *Phys Rev Lett* 1993;71:543.
- [2] Rosenfeld R, Feuerbacher M, Baufeld B, Bartsch M, Wollgarten M, Hanke G, et al. *Phil Mag Lett* 1995;72:375.
- [3] Wollgarten M, Bartsch M, Messerschmidt U, Feuerbacher M, Rosenfeld R, Beyss M, et al. *Phil Mag Lett* 1995;71:99.
- [4] Messerschmidt U, Geyer B, Bartsch M, Feuerbacher M, Urban K. *Mater Res Soc Symp Proc* 1999;553:319.
- [5] Feuerbacher M, Metzmacher C, Wollgarten M, Baufeld B, Bartsch M, Messerschmidt U, et al. *Mater Sci Eng A* 1997;233:103.
- [6] Takeuchi S, Tamura R, Kabutoya E. *Phil Mag A* 2002;82:379.
- [7] Messerschmidt U, Bartsch M. *Scripta Mater* 2003;49:33.
- [8] Caillard D, Vanderschaeve G, Bresson L, Gratias D. *Phil Mag A* 2000;80:237.
- [9] Caillard D, Roucau C, Bresson L, Gratias D. *Acta Mater* 2002;50:4499.
- [10] Caillard D, Morniroli JP, Vanderschaeve G, Bresson L, Gratias D. *Eur Phys J-Appl Phys* 2002;20:3.
- [11] Momprou F, Bresson L, Cordier P, Caillard D. *Phil Mag* 2003;83:3133.
- [12] Momprou F, Feuerbacher M, Caillard D. *Phil Mag* 2004 [in press].
- [13] Texier M, Prout A, Bonneville J, Rabier J, Baluc N, Cordier P. *Phil Mag Lett* 2002;82:659.
- [14] Cahn JW, Shechtman D, Gratias D. *J Mater Res* 1989;1:13.
- [15] Wollgarten M, Gratias D, Zhang Z, Urban K. *Phil Mag A* 1991;64:819.
- [16] Messerschmidt U, Bartsch M, Geyer B, Feuerbacher M, Urban K. *Phil Mag A* 2000;80:1165.
- [17] Benamara M, Rocher A, Sopéna P, Claverie A, Laporte A, Sarrabayrouse G, et al. *Mater Sci Eng B* 1996;42:164.
- [18] Yasutake K, Iwata M, Yoshii K, Umeno M, Kawabe H. *J Mater Sci* 1986;21:2185.
- [19] George A, Michot G. *Mater Sci Eng A* 1993;164:118.
- [20] Lawn BR, Hockey BJ, Wiederhorn SM. *J Mater Sci* 1980;15:1207.
- [21] Wiederhorn SM, Hockey BJ, Roberts DE. *Phil Mag* 1973;28:783.
- [22] Wollgarten M, Saka H, Inoue A. *Phil Mag A* 1999;79:2195.
- [23] Wollgarten M, Urban K. Dislocations and plasticity in quasicrystals. In: Hippert F, Gratias D, editors. *Lectures on quasicrystals*. Les Ulis: les éditions de physique; 1994. p. 535.